8-24-2009

Horizontal deviation of retinal nerve fiber layer peak thickness with Stratus optical coherence tomography in glaucoma

Jennifer Lee

Horizontal deviation of retinal nerve fiber layer peak thickness with Stratus optical coherence tomography in glaucoma

A Thesis Submitted to the

Yale University School of Medicine

in Partial Fulfillment of the Requirement for the

Degree of Doctor of Medicine

by

Jennifer Ching-Yi Lee

2009

HORIZONTAL DEVIATION OF RETINAL NERVE FIBER LAYER PEAK THICKNESS WITH STRATUS OPTICAL COHERENCE TOMOGRAPHY IN GLAUCOMA.

Jennifer C. Lee and M. Bruce Shields. Department of Ophthalmology and Visual Sciences, Yale University School of Medicine, New Haven, CT

We hypothesized that nasal or temporal peak contour shifts from the normative database observed on the Fast retinal nerve fiber layer (RNFL) scan is a common occurrence because there is a range of distribution of peak contours due to anatomical variation, not necessarily related to glaucoma, and this displacement may lead to misclassification as glaucoma under current commercial optical coherence tomography (OCT) criteria. The purpose of this study was to evaluate the prevalence these shifts with Stratus OCT and possible associations with demographic or glaucoma-related variables.

This was a retrospective case series of glaucoma patients and glaucoma suspects (one eye per patient) who underwent a Fast RNFL thickness study with the Stratus OCT. A study was considered to have a clinically significant horizontal deviation if there was greater than 20^o shift from the normative database in both superior and inferior peaks. A second cut-off value of 12^o was also used to examine smaller deviations. A linear regression model was used to assess correlations of demographic and glaucoma-related variables between eyes with and without significant deviations.

Of 400 subjects screened, 273 met the inclusion criteria. Thirty-nine eyes (14.3%) had clinically significant horizontal deviation using the 20^o cut-off (95%CI 10%-19%), while 122 (44.7%) met the definition with the 12^o cut-off (95%CI 38%-51%). Additionally, 121 eyes (44.3%) had a $>20^o$ horizontal shift of either the superior or inferior peak (95% CI 38%-51%). There was no correlation between the demographic or glaucoma-related variables and the horizontal deviation of peak contours.

This study suggests that significant horizontal deviation of peak RNFL contours with the Stratus OCT Fast RNFL is common and emphasizes the need for caution when interpreting the influence of such deviations on clock hour segment thinning. It is not possible with this technology to distinguish between scan circle misalignment (horizontal or vertical) and anatomical variation as the explanation for the finding, and further study with newer technology is needed.

Acknowledgements

This thesis was conducted in collaboration with Dr. M. Bruce Shields as the thesis advisor; without his expert knowledge, constant guidance and patience, this project would not have come to fruition. Pam Ossorio assisted with acquisition of OCT studies. Statistical analysis consultation was provided by Sunkyung Yu and James Dziura. This study was supported in part by a Yale University School of Medicine Medical Student Research Fellowship.

Table of Contents

Introduction

Glaucoma is a progressive optic atrophy, characterized by loss of retinal ganglion cells and tissue remodeling of the optic nerve head (Fig. 1). There are currently two main theories on the pathophysiology of glaucomatous optic neuropathy—a mechanical (pressure) and vascular (ocular blood flow) theory. The mechanical and vascular theories have been defended by various research groups since Smith in 1885 (1) first suggested that mechanical and vascular factors were involved in glaucoma pathogenesis (2).

Glaucoma was first described as a disease involving "firmness of the eyeball" and early physicians in the field considered increased intraocular pressure (IOP) the "essence" of glaucoma (2,3). According to the mechanical theory, increased intraocular pressure damages the laminar cribrosa by stretching the lamina beams and damaging the retinal ganglion cell axons, either directly by the pressure gradient or indirectly by tissue deformation (2,4). The presence of congenital glaucoma and angle-closure glaucoma indicate that increased IOP is sufficient to cause glaucomatous optic neuropathy. Furthermore, studies have shown a beneficial effect of eye pressure lowering therapy, even in normal tension glaucoma patients. Pressure lowering therapy, however, only slows the progression of glaucomatous optic neuropathy, and cannot reverse preexisting optic nerve damage or stop progression all together. In addition, normal tension glaucoma patients and patients with ocular hypertension but no glaucomatous nerve damage cannot be explained by the mechanical theory alone.

The vascular theory is based on the observation that a reduction of ocular blood flow often precedes the development of glaucomatous optic neuropathy. Ocular blood flow in patients with primary vascular dysregulation is irregular, leading to unstable

blood flow in the eye and mild repeated reperfusion injury via oxidative stress. The human eye can actually tolerate a constant reduction of blood flow (e.g. atherosclerosis, multiple sclerosis) to a certain level, without glaucomatous optic neuropathy, before an infarction occurs. It has been shown that fluctuating intraocular pressure is more damaging to the optic nerve head than a stable increase in intraocular pressure (5). Therefore, it is hypothesized that fluctuations in perfusion leads to oxidative stress (reperfusion injury) and eventually glaucomatous optic neuropathy (6).

Patients with systemic primary vascular dysregulation respond differently to stimuli and constrict their vessels more than others, including the vessels in the back of the eye (6). The theory that glaucoma is caused by a blood flow dysfunction is supported by data showing that blood flow is not only reduced in all areas of the eyes (iris, retina, optic nerve, choroids) in glaucoma patients but also in the capillaries of their fingers, pointing to a global vascular dysregulation. The insufficient autoregulation of blood vessels in the back of the eye reduces ocular blood flow leading to ischemia and reperfusion injury by reactive oxygen species, increasing the risk for glaucomatous optic neuropathy overtime (2).

In glaucoma patients, oxidative stress appears to play a dual role damaging both the trabecular meshwork and retina ganglion cells. Oxidative stress occurs when prooxidant induced damage exceeds the antioxidant repair capacity. Antioxidants are composed of enzymes, such as superoxide dismutase, gluthatione peroxidase and catalase, as well as molecules such as glutathione, flavonoids and vitamins C and E. It is thought that glaucoma patients have decreased antioxidant enzyme capacity in the aqueous humor as well as decreased plasmatic glutathione levels (7) which makes them

more susceptible to reactive oxygen species induced damage. One study showed that DNA damage is higher in the trabeular meshwork cells of glaucoma patients compared to age-matched controls (8).

Prior work on glaucoma pathophysiology assumed that the increased intraocular pressure observed in glaucoma patients is secondary to a decline in trabecular meshwork cellularity (9). The current thinking is that oxidative stress contributes to trabecular meshwork cellular degeneration, specifically the endothelial cells, which subsequently decreases aqueous outflow, and as a result causes increased intraocular pressure (10). A strong correlation between the degree of oxidative DNA damage in the trabecular meshwork and subsequent increased intraocular pressure and visual field defects has been shown in glaucoma patients with primary open-angle glaucoma (11). Thus, increased IOP in primary open angle is likely in part due to increased resistance to outflow through the trabecular meshwork (6).

Endothelins also appear to play a role in the regulation of intraocular pressure independent of the trabecular meshwork (10). Endothelin levels are elevated in the aqueous humor of glaucoma patients compared to healthy controls (12). Specifically, endothelin-1 appears to be the mediator in reducing optic nerve blood flow (13) leading to retinal ganglion cell death, independent of elevated intraocular pressure (14). Activation of endothelin receptors induces changes in the retinal ganglion cell axonal transport system leading to retinal ganglion cell apoptosis (10).

Unstable ocular blood flow in the retinal ganglion cells lead to oxidative stress and the production of oxygen free radicals. Ischemic stress activates astrocytes surrounding the optic nerve head which secrete nitric oxide (NO). When the secreted

nitric oxide (NO) combines with an oxygen free radical produced by the retinal ganglion cell, peroxynitrat ($ONOO^-$) is formed. The peroxynitrat ($ONOO^-$) diffuses into the retinal ganglion axons and lateral geniculate nucleus and induce apoptosis (6). Furthermore, there is a high concentration of mitochondria in the optic nerve head. Mitochondrial respiratory function declines with age and leads to increased production of oxygen free radicals by the mitochondria (15). Repeated mild reperfusion injury leads to chronic oxidative stress on the mitochondria, making them age faster and produce more oxygen free radicals, setting up a vicious cycle (6).

Aspects of both the mechanical and vascular theories interplay together in an individual patient to cause glaucomatous optic neuropathy. The mechanical theory was historically the original theory, but recent technological advances allowing measurement of ocular blood flow has yielded evidence that supports a vascular theory based on fluctuating ocular blood flow. The pressure theory alone does not explain normal tension glaucomatous optic neuropathy and why patients with ocular hypertension do not suffer glaucomatous optic neuropathy. There must be other mediating factors that make certain individuals more susceptible to damage by increased ocular pressure. Known glaucoma risk factors include myopia, sex, race, genetics, and autoimmune diseases (2). Differentiation between the two theories in practice is moot because the only widely available clinical treatments for glaucoma at present are ocular pressure lowering therapies. Perhaps with a better understanding of the pathophysiology of glaucoma, newer treatments will become available that target blood flow modulation or boost antioxidant repair capacity.

Abnormalities of the retinal nerve fiber layer (RNFL) are among the earliest signs of glaucomatous optic neuropathy (16). Visual field (VF) testing and stereoscopic optic nerve head (ONH) photography have traditionally been used to diagnose and follow glaucoma progression. However, retinal nerve fiber loss precedes visual field loss (17) and nearly half of the retinal ganglion cells in the retina may be lost before abnormalities in optic nerve head (ONH) appearance are noted (18,19). As retinal ganglion cells are lost, the retinal nerve fiber layer (RNFL) thins (20). Measurement of RNFL thickness has been shown to be more sensitive than visual fields or ONH photography in detecting early glaucoma (17,21).

There are currently three commercially available technologies for diagnostic imaging of the RNFL that is FDA approved for use in clinical practice: a confocal scanning laser ophthalmoscope (Heidelberg Retina Tomograph (HRT)), a scanning laser polarimeter (GDx) and an optical coherence tomograph (OCT). Each technology uses different properties of light and different characteristics of the retinal tissue to obtain RNFL thickness measurements. The models of each technology most studied in the literature will be reviewed in this paper, which are the HRTII (Heidelberg Engineering, Dossenheim, Germany), GDx Variable Corneal Compensation (VCC) (Carl Zeiss Meditec Inc., Vista, CA), and Stratus OCT (Carl Zeiss Meditec Inc., Dublin, CA) (Table 1, Table 2). Each instrument also includes an age-adjusted normative database for comparison (22) since RNFL thinning also occurs with aging. Furthermore, each technology has been shown to adequately differentiate normal eyes from glaucomatous eyes (23, 24, 25). There are more advanced models for each technology available, HRTIII, Cirrus HD-OCT and GDx (Enhanced Corneal Compensation (ECC)), but there

is very little evidenced-based literature available on the use of these models in clinical practice, and thus their clinical usage will not be discussed.

The ability of each technology to differentiate between normal eyes and glaucomatous eyes is often presented as the area under the receiver operator curve (AUROC) value, rather than sensitivity and specificity alone. The AUROC is a graphical plot of the sensitivity versus (1-specificity) for a binary classification system. This curve can also be represented equivalently by plotting the fraction of true positive (sensitivity) versus the fraction of false positives (1-specificity), however when presented this way, the value is referred to as the Relative Operating Characteristic (ROC) curve. The value for the AUROC ranges from 0.5 to 1, with 1 having the highest ability to discriminate between the two types of eyes.

Table 1: Differences between diagnostic imaging technologies for RNFL thickness measurements (28)

Instrument	Data obtained	Resolution	Best diagnostic parameter (AUROC)	Glaucoma prediction score	Cost
Stratus OCT	RNFL thickness around ONH	7-8μm	inferior RNFL (0.92)	None	~$61,950
GDx VCC	RNFL thickness around ONH	13μm	Nerve Fiber Indicator (0.91)	Nerve Fiber Indicator	~$47,950
HRT II	ONH and parapapillary topograph	11μm	linear discriminant function (0.86)	Glaucoma Probability Score	~$40,990

OCT optical coherence tomography; VCC variable corneal compensation; HRT Heidelberg Retina Tomograph; RNFL retinal nerve fiber layer; ONH optic nerve head, AUROC area under the receiver operator curve

Table 2: Pros and Cons between diagnostic imaging technologies for RNFL thickness measurements

Instrument	Pros	Cons
Stratus OCT	Ability to differentiate between layers of the retina, retina and glaucoma applications	Operator drawn optic-disc margin, RNFL thickness limited to circle around ONH and not parapapillary region, requires pupil dilation, no progression analysis
GDx VCC	No pupil dilation	Atypical birefringence pattern in older patients, irregularities in cornea or macular architecture can alter retardation, only measures RNFL thickness
HRT II	Parapapillary retina tomographic map	Operator drawn optic-disc margin, magnification correction, reference plane

OCT optical coherence tomography; VCC variable corneal compensation; HRT Heidelberg Retina Tomograph; RNFL retinal nerve fiber layer; ONH optic nerve head

ONH diagnostic imaging technologies

Scanning laser polarimetry (GDx) (26):

Scanning laser polarimetry (SLP) utilizes reflected polarized light (780nm) undergoing a phase shift (retardation) corresponding to the amount of birefringent tissue (neurotubules within ganglion cell axons) passed in the retina, which is proportional to the thickness in the retinal nerve fiber layer (22). Since SLP is measuring RNFL

thickness proportionally, it is susceptible to confounding birefringence by non-RNFL structures in the eye (mainly from the cornea). Therefore it is necessary to compensate for the birefringence of these structures in order to reduce interference with RNFL thickness measurements. Newer models of SLP (GDx VCC) have better algorithms to compensate for corneal birefringence. Most recently, the GDx ECC provides individual compensation for corneal birefringence. The RNFL Temporal-Superior-Nasal-Inferior-Temporal (TSNIT) profile is generated from a 3.2mm calculation circle centered on the ONH (27), but the nerve fiber indicator (NFI), value (from 0 to 100) representing the likelihood of glaucoma diagnosis, is based on the entire RNFL thickness map. Among the various standard GDx VCC parameters, the NFI parameter has the best diagnostic accuracy with AUC values ranging from 0.89 (preperimetric) to 0.94 (perimetric loss) (27, 28,29). RNFL contour measurements are compared to a normative database to determine areas of change.

Confocal scanning laser ophthalmoscopy (CSLO) (HRT) (30):

The CSLO utilizes a diode laser (670 nm wavelength) to sequentially scan the retinal surface in the x and y plane at 64 consecutive equidistant focal planes along the z-axis (optic nerve axis) to create a three-dimensional topographic map of the retinal surface which provides calculations of peripapillary retinal height measurements and cup-to-disc ratio. RNFL thickness around the ONH is calculated by measuring the distance between the mean height contour and an individual based reference plane, as this instrument does not different between layers of the retina (22). Surface height aberrations relative to a normative database are highlighted. The HRTII printout includes

the glaucoma probability score (GPS), which combines five parameters (two RNFL parameters and three optic disc parameters) to provide the probability of having glaucoma (Fig. 2). Using the HRT I, Zanwill et al. (23) found the AUROC ranged from 0.75 to 0.96.

Optical Coherence Tomography (OCT) (30):

OCT uses low-coherence laser interferometry (850nm) to examine light backscattered from individual layers of the retina with differing optical densities, which is analogous to ultrasound imaging except using light instead of sound. This technology can differentiate between layers of the retina using edge detection algorithms to give RNFL thickness measurements. The Stratus OCT Fast RNFL scan provides 3 scans, each scan includes 256 equally spaced A-scans (2 dimensional axial cross-sectional image) along a 360^{o} scan circle (3.4mm) centered around the ONH. The RNFL values are compared to an aged-matched normative database and deviations reported as sectoral thinning (Fig. 3).

RNFL inferior thickness and average thickness have the best diagnostic accuracy of the Stratus OCT RNFL measurement parameters (28, 32). Combining the results from multiple studies correlating glaucoma diagnosis with OCT RNFL measurements, mean RNFL thickness in the superior and inferior quadrants had the highest AUROC with 0.79 to 0.95 for the superior quadrant and 0.86 to 0.97 for the inferior quadrant (27, 33, 34, 35). AUROC values comparing glaucoma suspects with controls were lower than the values of glaucoma patients with VF loss, ranging from 0.59 to 0.84 for the superior quadrant and 0.69 to 0.81 for the inferior quadrant (27, 33, 34, 35).

The newest commercially available version of OCT is spectral domain(SD)-OCT (Cirrus HD-OCT, Carl Zeiss Meditec, Inc. Dublin, CA) which has much faster scanning, better axial resolution, and eliminates the need for operator centering of the ONH compared to the previous time domain (TD)-OCT (Stratus OCT) (Table 3). SD-OCT collects all the backscattered light frequencies simultaneously (hence "spectral domain"). This version uses a broad bandwidth light source to achieve low coherence. Since each frequency of light represents a different tissue depth, the frequencies of reflections can be mapped to individual retinal layers (20). The SD-OCT algorithm creates a virtual 3.4mm scan circle around the ONH after processing the scan data, allowing for precise centration of the scan circle around the ONH. Furthermore, decreased acquisition time reduces motion artifact from minuscule eye movements during scanning. One possible explanation for variable measurements obtained with TD-OCT is varying placement of the scan circle around the ONH, giving slightly different measurements each time. Spectral domain technology should overcome this problem and allow for more consistent scans.

Table 3: Time domain OCT versus Spectral domain OCT (20)

Version	Resolution	A-scans/second	Scan circle placement	A-scan timing relative to ONH centering
Time domain	10-15μm	400	Operator center disc margin	Immediately before
Spectral domain	3-6um	24,000-55,000	Virtual via algorithm	Simultaneous

OCT optical coherence tomography; ONH optic nerve head

Comparison of the three RNFL imaging technologies:

There are a number of barriers to directly comparing diagnostic accuracy between the three imaging technologies. A limited number of published studies exist that compare multiple imaging modalities in the same patient (28, 36, 37, 38, 39, 40, 41). Furthermore, it is problematic comparing results across different studies because there are varying criteria for glaucoma diagnosis (e.g. glaucomatous VF defect versus glaucomatous change in the optic disc) and varying degrees of glaucoma severity in each study.

Studies comparing HRT versus GDx VCC and OCT versus HRT showed good intra-instrument correlation (40, 41), however the values are not interchangeable between instruments (27, 38). One study comparing Stratus OCT and GDx VCC found that OCT RNFL values correlated with visual function better than GDx VCC RNFL values in regression analysis (34). Furthermore, the same study found Stratus OCT RNFL thickness values to be significantly greater than GDx VCC RNFL thickness values in

both normal and glaucoma eyes (39). Despite this difference however, the best diagnostic parameter for each instrument had equal AUROC values (0.901 for Stratus OCT and 0.909 for GDx VCC) (39). A study by Schuman et al. (41) found similar AUROC values for Status OCT and HRTI.

At present, there is only one study directly comparing all three technologies. In this study, Medeiros et al. (28) found no significant difference in the diagnostic accuracy (AUROC) of the best parameters for each technology: GDx VCC (Nerve Fiber Indicator) 0.91, Stratus OCT (inferior quadrant) 0.92 and HRTII (linear discriminant function) 0.86 (Table 1). Therefore, with the current algorithms, no one imaging device does better than the other available technologies in distinguishing glaucoma patients from control subjects and in predicting glaucoma progression. SLP (GDx) is less commonly used than HRT and OCT in clinical practice because its clinical applicability is limited to measuring RNFL thickness. However, the GDx and HRT both provide glaucoma likelihood values (i.e. Nerve Fiber Indicator for GDx and Glaucoma Probability Score for HRT) which may be useful clinically. Newer versions of the present technologies and better algorithms on the horizon are likely to provide better resolution, diagnostic accuracy, and progression analysis.

Utility of diagnostic imaging in predicting the development of glaucoma or progression analysis:

There have only been a handful of longitudinal studies on the ability of diagnostic imaging of the RNFL to predict the development of visual field changes or document thinning of the RNFL consistent with visual field progression (42, 43, 44). A major

barrier to conducting longitudinal prospective studies is the rapidly evolving technology and the inability to compare (incompatible) measurements between different versions of the same technology. Glaucoma, a chronic progressive disease, requires longitudinal follow-up with a standardized baseline measurement for comparison. Clinical practitioners agree that disease progression analysis is crucial to the management of glaucoma.

A number of studies have reported the ability of HRT to document glaucoma progression using topographic change analysis within the disc margin (45, 46, 47). Topographic change analysis compares the baseline ONH topograph with subsequent scans. According to the Confocal Scanning Laser Ophthalmoscopy (CSLO) ancillary study to the Ocular Hypertension Treatment Study (OHTS), abnormal mean height contour HRTII measurements at baseline have been associated with the development of glaucomatous optic disc and visual field progression in ocular hypertensive eyes without optic disc or visual field damage at baseline (46). Two longitudinal prospective studies using HRTI followed glaucoma patients who had glaucomatous VF loss at baseline measuring optic disc changes, standard automated perimetry (SAP) and high-pass resolution perimtery. The authors found a large number of patients progressed by perimetry or HRT alone (42, 43). Of note, the HRTIII model has backward compatibility, which means it is able to incorporate ONH measurements from prior models, and therefore progression analysis studies with the HRTIII are forthcoming. At present, HRT RNFL measurements alone have not been shown to predict the development of glaucoma (only the baseline ONH topograph).

A longitudinal study using a prototype OCT model on glaucoma patients and glaucoma suspects showed a greater likelihood of glaucomatous progression identified by OCT (arbitrarily defined as change of 20 μm) compared with automated perimetry (arbitrarily defined as 2 dB MD) over a 4.7 year period (44). It is unclear, however, whether these detected changes reflect OCT false positive (hypersensitivity) results or glaucomatous damage identified by OCT before detection by conventional methods (SAP or clinical assessment). The authors also found a portion of patients that progressed by OCT (21.9%) or VF (9.4%) alone.

Currently there are no studies available on the ability of baseline GDx VCC or Stratus OCT RNFL measurements to predict the development of glaucoma or identify the progression of disease. The RNFL baseline measurement in an older version of the GDx Nerve Fiber Analyzer with fixed corneal compensation was predictive of the development of visual field loss in glaucoma suspect eyes (48). Similarly, thinner (10μm average) superior and inferior baseline RNFL measurements in a prior OCT model was associated with the development of glaucomatous change (VF damage or optic neuropathy) in glaucoma suspects over a 4 year period (49). Glaucoma progression analysis software is currently being developed and tested for the Stratus OCT using trend analysis and event analysis.

The only validated model that estimates the 5 year risk of conversion from ocular hypertension to glaucoma derived from the Ocular Hypertension Treatment Study (50) does not include RNFL measurements derived from peripapillary imaging. The demographic and clinical factors included in the model are age, race, sex, intraocular pressure, central corneal thickness, diabetes mellitus diagnosis, vertical cup-disc ratio,

horizontal cup-disc ratio and VF pattern standard deviation. This same model was applied to a different untreated cohort in the Diagnostic Innovations in Glaucoma Study with similar results except for the presence of diabetes mellitus (51).

Does use of diagnostic imaging improve disease management or diagnosis?

At present, diagnostic imaging of the optic nerve and peripapillary RNFL is only used as an adjunct to VF testing and ONH stereophotography for glaucoma diagnosis and management. There is widespread use of peripapillary imaging in glaucoma without clear evidence as to whether diagnostic imaging actually improves disease management or early diagnosis. Diagnostic imaging can provide additional information not available via ONH photography, such as objective quantitative structural measurements of the peripapillary RNFL, but the present versions of these technologies are not sufficient to replace ONH photography for following glaucoma progression.

There are many potential utilities of diagnostic imaging as the technology continues to improve. Given the inherent variability in clinician ONH drawings and interpretation of ONH stereophotography, RNFL imaging can provide an objective documentation of baseline quantitative peripapillary RNFL measurements which can then be referenced in subsequent office visits. In addition, diagnostic imaging allows comparison of a patient's RNFL measurements with an aged-matched normative database (since thinning also occurs with aging). RNFL abnormalities occur in early glaucoma before VF changes noted on standard automated perimetry (SAP) (52). RNFL thinning may be the earliest structural change clinically detectable as RNFL thinning has been shown to occur as early as 6 years before VF loss (53).

Glaucomatous changes may initially be subtle, and diagnostic imaging can provide more sensitive measures of RNFL changes which may lead to earlier diagnosis of glaucoma suspects, before changes are noted on VF testing and ONH photography. Two studies on glaucoma progression both showed higher rates of glaucoma progression using RNFL structural analysis compared to standard automated perimetry (SAP); 44%-82% by HRT versus 33%-57% by SAP and 25% by OCT versus 12% by SAP respectively (43, 44). Another important potential usage of diagnostic imaging is to objectively quantify glaucoma progression and predict VF changes. Progression analysis software is currently under development for each technology. Theoretically, diagnostic imaging can detect subtle changes in the RNFL in a shorter period of time, however, there are not enough longitudinal studies to support this claim.

The current gold standard for glaucoma diagnosis is documented VF change and ONH thinning observed on stereoscopic photography, which is a crude measure of RNFL damage. With more sensitive measures of RNFL thickness allotted by imaging, rather than waiting for VF changes or ONH thinning, clinicians may need to reconsider the criteria for glaucoma diagnosis. If they lower their threshold for starting medical treatment, they may be able to prevent progression to VF changes. Relying on imaging for diagnosis, however, can give false positive results and result in over-treatment of glaucoma suspects. It is standard practice to obtain 3 abnormal VF results before giving the diagnosis of glaucoma, but there is no common standard in imaging to perform repeat imaging to establish a baseline RNFL measurement. Furthermore, all imaging technologies assume the patient has a normal retina because their measurements are compared to a normative database. If a patient has an abnormal retina, they will

inherently have abnormal RNFL measurements when compared to the normative database. Consequently, clinicians should not base treatment decisions on one imaging result and should ensure the results fit with the clinical picture (i.e. structure-function concordance). A major draw back of RNFL imaging is that none of the current technologies allow for the detection of optic disc hemorrhage (54), thus ONH photography remains a crucial part of glaucoma management.

Studies have shown good agreement between RNFL measurements and VF testing and ONH photography. There are many cases, however, where peripapillary imaging suggestive of glaucomatous changes are not correlated with VF changes or damage on ONH photography (i.e. structure-function discordance) (42, 43, 44). This discrepancy may be indicative of early glaucoma, false positive results or independent predictors of glaucoma (22, 27). Furthermore, there are a number of cases where observed VF or ONH damage resulted in normal RNFL measurements in the same patient (42, 43). These inconsistencies raise questions whether diagnostic imaging measures different retinal ganglion cell properties than those measured in functional VF testing (55) (Table 4). Diagnostic imaging provides objective quantitative assessment of the peripapillary structure and the cup-to-disc ratio while VF testing gives functional assessment of the optic nerve and fundus photography provides qualitative assessment of ONH cupping (the width of nerve fiber loss). Therefore, the three test results may not exactly correlate, giving rise to observed structure-function discordance. These discrepancies raise the question of whether early structural damage detected by RNFL imaging analysis will eventually lead to functional loss, as theorized.

Table 4: Optic disc photography versus RNFL imaging

	Type of measurement	Type of assessment	Detect hemorrhages	Detect progression	Early glaucoma
ONH photography	subjective	qualitative	Yes	Yes	No
RNFL imaging[A]	objective	structural	No	potentially	potentially

[A]GDx VCC, HRTII, Stratus OCT

Purpose of study:

There is increasing use of computerized image analysis of the RNFL, especially OCT, to aid in the diagnosis and management of glaucoma, highlighting the need for accurate interpretation of the results of this evolving technology. The Stratus OCT Fast RNFL scan provides a normative database with thickness percentile values of normal eyes, against which the patient's RNFL thickness contour is compared (56). Contours that approach or pass the $<5^{th}$ percentile (yellow zone) are viewed with suspicion as abnormally thin RNFL. If the superior or inferior peak contour is displaced nasally or temporally from that of the normative database, for whatever reason, one slope of the contour may cut into the $<5^{th}$ percentile, suggesting RNFL thinning, even though the amplitude of the peak contour may be well within the 95^{th} percentile (Fig. 4). This could represent true thinning or could result from misalignment of the scan circle or possibly from a variation in the patient's anatomy, e.g., a deviation from the average in the axis of

peak RNFL thickness. To our knowledge, this potential source of misinterpreting OCT findings ("technology created glaucoma") has not been emphasized in the literature.

We hypothesized that nasal or temporal peak contour shifts from the normative database observed on the Fast RNFL scan is a common occurrence because there is a range of distribution of peak contours due to anatomical variation, not necessarily related to glaucoma, and this displacement may lead to misclassification as glaucoma under current commercial OCT criteria (comparing an individual's RNFL measurements to a normative database) resulting in over aggressive treatment for glaucoma.

The purpose of this study was to evaluate how common significant horizontal peak contour shifts with the Stratus OCT Fast RNFL may be in a practice with glaucoma patients and glaucoma suspects, to explore whether demographic or glaucoma-related variables are associated with this finding and to emphasize the importance of this finding when interpreting the data.

Materials and Methods:

This was a retrospective case series of consecutive patients seen at the Yale Eye Center, Department of Ophthalmology and Visual Science, New Haven, CT. The inclusion criteria were glaucoma patients and glaucoma suspects who underwent a Stratus OCT Fast RNFL study between October 2007 and August 2008. Exclusion criteria comprised of patients under 20 years of age (normative database is not available below this age), a superior or inferior peak contour amplitude < 100μm (peak of the contour is difficult to identify below this amplitude), signal strength of less than 6 (analysis algorithms may fail on scans with low signal strength <5), and poor scan circle centration (>50% difference between edge of the optic disc and scan circle, temporally and nasally, as well as superiorly and inferiorly) (i.e. translational misalignment). One eye from each subject was selected for analysis using the "random sample of cases" function in SPSS, although both eyes were studied to determine bilaterality of findings, and the most recent test was chosen for patients who had more than one test. The study was approved by the Yale University Human Investigation Committee and conforms to the Declaration of Helsinki research on human subjects and HIPPA.

A Stratus OCT 3000 system (Carl Zeiss Meditec, Dublin, CA) with the Fast RNFL scan pattern and Stratus software version 4.0 was used to obtain the circumpapillary RNFL thickness profile. Details of this system are described elsewhere (31, 56, 57). The patient's RNFL is differentiated from other retinal layers using an edge detection algorithm (version A4X1), and the RNFL thickness for 360º around the disc (scan circle diameter of 3.4 mm) is defined as the number of pixels between its anterior and posterior boundaries. Three consecutive scans, centered on the optic disc, are

averaged for each eye to produce the thickness report. The RNFL thickness report includes the fundus image and scan circle centration, peripapillary retinal cross section image, and RNFL thickness profiles against age stratified normal values derived from manufacturer averages of healthy eyes (Fig. 3). However, the exact times at which the scan circle centration image and the thickness profiles were acquired were not simultaneous.

An experienced technician centered the scan circle around the optic disc and obtained the Fast RNFL studies. One of us (JCL) evaluated each study on a digital monitor, assessing signal strength, scan circle centration, amplitude and horizontal position of the superior and inferior peak contours against the aged-matched normative database. The horizontal distance between the peaks of the patient's RNFL profile and that of the normative database was measured digitally using EyeRoute software (Topcon Medical Systems, Inc., Paramus, NJ) which allows measurement of distances in mm, which we then converted to degrees. Each horizontal sampling segment (distance between tick marks along the x-axis) comprised of 10 A-scans (total 256 A-scans equally spaced along the 360^{o} scan circle) was 1.2mm, which is equivalent to a 14^{o} shift (360^{o}*10/256) (Fig. 5). A significant horizontal shift of the peak contour was defined as 20^{o} (1.7mm) or greater nasal or temporal to the corresponding peak contour of the normative database. This cut-off value was selected because it is likely to be associated with one slope of the RNFL contour falling into the $<5^{th}$ percentile zone. An eye was considered to have a clinically significant horizontal deviation if there was a 20^{o} or greater shift of both the superior and inferior peaks (Fig. 5). A second cut-off value of 12^{o} (1.02mm) or more was also used to examine smaller deviations.

Subjects who met the inclusion-exclusion criteria, but did not have significant horizontal deviation in either eye, were randomly selected (using the "random sample of cases" function in SPSS) as controls for comparing demographic and glaucoma-related variables between eyes with and without significant horizontal deviation. Demographic variables studied were age (years), race (Caucasian, African American and other) and sex, while glaucoma-related variables included cup-disc ratio (C/D), neural rim (even, focal thinning or focal absence) and pattern standard deviation (PSD) obtained from a Humphrey SITA 24-2 visual field. The C/D was derived from ophthalmoscope examination measured vertically and calculated as a ratio of the diameters. Fisher exact χ^2 tests were used to compare the categorical variables (sex, race and neural rim) between eyes with and without significant horizontal deviation, as well as the direction of peak contour shift (temporal vs. nasal) in those eyes with significant deviation. Mann-Whitney U t-tests were used to compare the continuous variables (age, C/D and PSD) between eyes with and without significant horizontal deviation. A linear regression, including the variables of age, race, sex, C/D, neural rim and PSD, was performed using the "enter" method, in which all variables in a block are entered in a single step into the model. Level of significance was set with α=0.05. SPSS V14.0 was used for statistical analysis.

This study design was a joint collaboration between MBS and JCL. JCL prepared HIC forms, collected clinical data, performed statistical analysis of data, and prepared the manuscript. Pam Ossario from the Department of Ophthalmology and Visual Sciences assisted with the acquisition of OCT studies.

Results

Of 400 subjects screened, 273 subjects met the inclusion and exclusion criteria. Thirty-nine of the 273 eyes met the criteria for significant horizontal contour deviation using the 20^o cut-off value, giving a prevalence of 14.3% (95%CI 10%-19%), while 122 subjects had significant deviation with the 12^o cut-off, increasing the prevalence to 44.7% (95%CI 38%-51%). Bilateral significant deviation was seen in four subjects using the 20^o cut-off and in 18 with the 12^o cut-off. An additional 121 subjects had a significant horizontal shift (20^o) in either the superior or inferior peak, giving a prevalence of 44.3% (95%CI 38%-51%), with 48 superior shifts and 76 inferior. Seven of these 121 subjects had bilateral significant shifts (20^o) in the superior quadrant and 14 in the inferior quadrant, while three subjects had a superior shift in one eye and an inferior shift in the fellow eye (resulting in 124 significant shifts in 121 subjects).

Tables 5 and 6 show the prevalence of the direction of superior and inferior peak contour shifts and the average and range of the shifts in degrees for the 39 subjects that met the criteria for significant horizontal deviation at the 20^o cut-off. Tables 7 and 8 show the same information for the 122 subjects that met the criteria at the 12^o cut-off. The direction of peak shifts in eyes that met the 20^o cut-off was nasal in 20, temporal in 13 and mixed (one peak temporal and one nasal) in 6 eyes ($p=0.02$), while that for the eyes meeting the 12^o cut-off was more evenly distributed with 45 nasal, 40 temporal and 37 mixed ($p=0.67$).

Table 5: Horizontal shift distribution with 20^o cut-off.

	Number of eyes	% [A]	%[B]	p value
Nasal	20	7.3%	51.3%	0.02 (χ^2)
Temporal	13	4.8%	33.3%	
Mixed[C]	6	2.2%	15.4%	
Total	39	14.3		

[A]percentage in total population (n=273)

[B]percentage of significant horizontal deviations (n=39)

[C]one peak (superior or inferior) was displaced nasally and the other temporally

Table 6: Mean and range of horizontal shifts in eyes with significant deviation ($\geq 20^o$) [A].

	Number of subjects	Minimum Shift (^{o})	Maximum Shift (^{o})	Mean Shift (^{o})	Std. Deviation (^{o})
Superior peak Nasal shift	25	20.0	83.4	34.1	18.6
Superior peak Temporal shift	14	20.0	57.6	31.8	10.3
Inferior peak Nasal shift	21	21.2	50.3	32.1	8.6
Inferior peak Temporal shift	18	20.0	50.3	31.8	10.1

[A]20^o or more shift nasal or temporal to the corresponding peak contour of the normative database in both the superior and inferior peaks

Table 7: Horizontal shift distribution with 12^o cut-off.

	Number of eyes	% [A]	%[B]	p value
Nasal	45	16.5%	36.9%	0.67 (χ^2)
Temporal	40	14.7%	32.8%	
Mixed[C]	37	13.6%	30.3%	
Total	122	44.7%		

[A]percentage in total population (n=273)

[B]percentage of $\geq 12^o$ horizontal deviations (n=122)

[C]one peak (superior or inferior) was displaced nasally and the other temporally

Table 8: Mean and range of horizontal shifts in eyes with $\geq 12^o$ deviation[A].

	Number of Subjects	Minimum Shift (^{o})	Maximum Shift (^{o})	Mean Shift (^{o})	Std. Deviation (^{o})
Superior peak Nasal shift	74	12.9	83.4	25.1	14.3
Superior peak Temporal shift	48	12.9	57.6	23.5	9.8
Inferior peak Nasal shift	53	12.9	51.5	26.4	10.1
Inferior peak Temporal shift	69	12.3	50.3	23.4	10.0

[A]12^o or more shift nasal or temporal to the corresponding peak contour of the normative database in both the superior and inferior peaks

When comparing eyes with and without significant horizontal deviation (20^o), there was no significant difference in the direction of the shifts between the two groups (Table 9).

Table 9: Direction of shifts in subjects with and without significant deviation[A]

	Significant Deviation (n=39)	Non-significant Deviation (n=39)	p value
Superior (nasal)	64.1%	64.4%	1.00 (χ^2)
Inferior (nasal)	53.9%	40.0%	0.27 (χ^2)

[A]20^o or more shift nasal or temporal to the corresponding peak contour of the normative database in both the superior and inferior peaks

Furthermore, there was no statistically significant difference in demographics variables or glaucoma-related variables (Table 10) between eyes with and without significant horizontal deviation. The presence of a significant horizontal deviation did not correspond with glaucoma diagnosis when using optic nerve head thinning as the "gold standard", as evidenced by the high false positive rate (49%) and false negative rate (58%) observed (Table 11). A linear regression model incorporating the demographic and glaucoma-related variables revealed no significant factors.

Table 10: Comparison of demographics and glaucoma-related variables in subjects with and without significant deviation[A]

	Significant Deviation (n=39)	Non-significant Deviation (n=39)	p value
Age (years, SD)	64.0 (14.1)	65.9(13.4)	0.52 (t-test)
Female	64.4%	64.1%	1.00 (χ^2)
Caucasian	78.1%	73.0%	0.42 (χ^2)
African American	14.6%	21.6%	
Neural rim (even)	66.7%	60.0%	0.17 (χ^2)
C/D (SD)	0.60 (0.17)	0.64 (0.16)	0.33 (t-test)
PSD (SD)	3.63 (2.92)	2.80 (2.23)	0.15 (t-test)

SD (standard deviation), Neural rim (graded even, focal thinning or focal absence), C/D (cup-disc ratio), PSD (pattern standard deviation)

[A]20^o or more shift nasal or temporal to the corresponding peak contour of the normative database in both the superior and inferior peaks

Table 11: False positive and false negative rates in subjects with and without significant deviation[A]

	Glaucoma[B]	Glaucoma suspect
(+)shift	13	26
(-)shift	18	27
Total	31	53

false positive rate= 49%

false negative rate= 58%

[A]Positive clinical test based on significant deviation of 20^0 or more shift nasal or temporal to the corresponding peak contour of the normative database in both the superior and inferior peaks

[B]"Gold standard" for glaucoma diagnosis based on optic nerve head neural rim thinning (either focal thinning or focal absence)

Discussion

The diagnostic accuracy of the imaging derived RNFL measurements is generally good in differentiating glaucoma from normal eyes with no significant difference between the best parameters of each instrument (HRT, GDx, OCT). There are varying AUROC values reported for each instrument due to the range of criteria used for glaucoma diagnosis, the patient population (control, ocular hypertensive or glaucoma), and the specific algorithm used for analysis in each study. Since glaucoma remains a clinical diagnosis, it will be difficult to reach consensus criteria for glaucoma diagnosis. The advantage of OCT is that it directly measures RNFL thickness, while GDx and HRT indirectly measure RNFL thickness. However, the GDx and HRT both provide glaucoma likelihood scores which have great clinical utility.

With multiple technologies available, it is important that the ophthalmologist understand the strengths and weaknesses of each type of instrument and the type of data provided in order to correctly interpret the relevant data from the test results and appropriately integrate the information into glaucoma management. The influence of scan circle misalignment on both the amplitude and horizontal position of RNFL thickness peak contours in relation to the normative database has been described with the Stratus OCT (58, 59) and with ultrahigh-resolution OCT (60). A vertical misalignment can cause the amplitude of one peak, i.e., superior or inferior, to be artificially elevated, while the opposite quadrant is artificially reduced. For example, if the scan circle is misaligned superiorly, i.e., the circle is closer to the inferior edge of the ONH, the superior peak will be artificially reduced and the inferior artificially elevated. A horizontal misalignment of the scan circle will influence the horizontal positions of the

peak contours in relation to that of the normative database. Nasal misalignment, i.e., with the circle closer to the temporal edge of the ONH, is associated with a temporal shift of the peak contours, while temporal misalignment leads to a nasal shift of the peaks (59, 60).

While horizontal shift of RNFL thickness peak contours in relation to that of the normative database is known to be a potential artifact with the Stratus OCT Fast RNFL study, we are not aware of an emphasis in the literature on the importance of this finding with regard to interpretation of the data nor how often it may be seen in clinical practice. The purpose of our study and report is to address these latter issues.

A significant horizontal shift of a contour peak can influence the interpretation of the data, since one slope of the contour may cut into the $<5^{th}$ percentile of the database, suggesting abnormal RNFL thinning in that area, despite a peak amplitude that is well within the 95^{th} percentile. In some cases, this could represent true, focal RNFL thinning, while in other cases, the shift may be an artifact due to misalignment of the scan circle, as described above, which could create a false impression of thinning (technology created RNFL thinning). Another as yet unproven, explanation for the contour shift could be an anatomical variation from the average in the axis of a person's peak RNFL thickness in the superior-temporal and inferior-temporal quadrants. Such variations might produce horizontal shifts of peak contour large enough to create a false impression of RNFL thinning in healthy eyes. We are unable to substantiate this theoretical explanation in our present study, because the Stratus OCT system records the image of the scan circle over the ONH immediately after acquiring the RNFL thickness data. Therefore, although we excluded cases with gross decentration of the scan circle on the available image, we

could not rule out the possibility of miniscule eye movements as the explanation for the cases in which significant horizontal shift of the peak contours were noted.

Our study, therefore, was limited to assessing the prevalence with which significant horizontal deviation may occur, from whatever cause, with the Stratus OCT Fast RNFL scan in glaucoma patients and glaucoma suspects and to evaluating whether this finding is associated with certain demographic or glaucoma-related variables. We found horizontal contour deviation to be common in our patients. When defining a significant deviation as 20^{o} or more either nasal or temporal to that of the normative database in both the superior and inferior contour peaks, the prevalence was 14.3% (95% CI 10%-19%). We chose this cut-off value, because it usually caused the RNFL thickness contour to cut into the $<5^{th}$ percentile of the normative database. We also looked at a lower cut-off of 12^{o} or more, which increased the prevalence to 44.7% (95%CI 39%-51%). With the larger cut-off, the majority (51%) of eyes had a nasal shift, while eyes with the smaller cut-off were more evenly distributed between nasal and temporal shifts. An additional 44.3% (95%CI 38%-50%) of eyes had a significant shift (20^{o} or more) in either the superior (48) or inferior (76) peak contour. Only a minority of subjects had significant horizontal shifts of both peaks bilaterally, and there was no significant correlation with demographic (age, race or sex) or glaucoma-related (C/D, neural rim or PSD) variables between eyes with and without significant horizontal deviation. Furthermore, the presence of a significant horizontal deviation did not differentiate between glaucoma and glaucoma suspect subjects.

Our findings are consistent with those of Ghadiali et al. (61), who found wide variation in the shape of the RNFL profiles and location of the peaks, which was not

associated with age, refractive error or signal strength, although they found better correlation of RNFL profiles between eyes than in our study. These authors also suggested that a variation in pattern of axons or possibly in blood vessel location might account for the variable RNFL profile pattern.

Supporting the theory of anatomical variation, as a partial explanation for the horizontal shift of contour peak, was the observation in our study that the majority of shifts of 20^{o} or more were in the nasal direction. If the shifts were all due to scan circle misalignment (either operator error or miniscule eye movements), it is likely that this would be random with a more even distribution in the direction of peak shifts. The fact remains, however, that the influence of circle misalignment cannot be ruled out with the Stratus OCT, since the image of the scan circle over the ONH and the RNFL thickness data are not acquired simultaneously. While horizontal shift of the RNFL contour is associated with the quadrant and average RNFL thickness, we did not attempt to quantify this correlation. In addition, we only considered the possible influence of translational misalignment of the circle scan (i.e., horizontal or vertical) and not rotational shifts of the eye on horizontal deviation.

A limitation of our study, therefore, was the inability to rule out scan circle decentration as the explanation for the horizontal deviation in peak contours. Even though we excluded eyes with gross scan circle misalignment, it is possible that sudden small eye movement between acquisition of the scan circle/ONH image and the actual OCT scan could have caused an undetected decentration of the ONH. Our study does, however, suggest that significant horizontal deviation of peak contours is common with the Stratus OCT Fast RNFL scan in glaucoma patients and glaucoma suspects, and

emphasizes the need for caution when interpreting the influence of horizontal deviation on clock hour segment thinning reported by Stratus OCT.

The findings in the present study may not be applicable to the next generation of spectral domain OCT, such as the Cirrus-HD OCT, which eliminates the need for operator centering of the ONH and allows for precise centration of the scan circle around the ONH. The algorithm with this technology creates a virtual 3.4mm scan circle around the ONH after processing the scan data, and the decreased acquisition time will reduce motion artifact from minuscule eye movements during scanning. Further study, therefore, is needed to establish the prevalence of horizontal peak contour deviation with this newer technology and to better understand the mechanism behind it.

A problem with the interpretation of the RNFL thickness results of current models is that there is a wide range in the number of retinal ganglion cells in the normal population and thus there is considerable overlap in RNFL measurements between normal eyes and eyes with early to moderate glaucoma. Similarly, there is probably a wide variation in the location of the peak contours observed in the superior and inferior quadrants. As a result, the ability to diagnose early RNFL damage may dependent on the ability to detect small RNFL thinning from baseline in each individual patient over time, rather than comparison to a normative database (as is current practice). There are, however, very few longitudinal studies evaluating small changes in RNFL thickness measurements that may predict development of glaucoma or monitor its progression.

For now, RNFL measurements are only used as an adjunct to ONH photography and VF testing to aid in glaucoma management. A report put out my the American Academy of Ophthalmology on RNFL analysis technology in 2007 (27) stated that

"information obtained from imaging devices is useful in clinical practice when analyzed in conjunction with other relevant parameters that define glaucoma diagnosis and progression." The "gold standard" for glaucoma diagnosis remains intraocular pressure measurement, standard automated perimetry(SAP) and ONH photography. There are inherent problems with the current "gold standard" measurements for glaucoma diagnosis. Interpretation of ONH photographs is subjective and VF testing is highly variable depending on subject performance, while RNFL imaging measurements, based on a preprogrammed algorithm, are objective. The ability of RNFL progression analysis to detect small changes in RNFL structure before SAP is promising for future early detection of glaucoma progression. Current utilities of RNFL imaging include early diagnosis of glaucoma and documentation of baseline measurements, but VF testing and ONH photography remain the mainstays of following glaucoma progression.

Most of the published studies thus far have focused on the ability of diagnostic imaging to differentiate between normal eyes and glaucomatous eyes that have documented VF defects. The real utility of diagnostic imaging in clinical practice lies in the ability to detect early RNFL damage in glaucoma suspects before there is detectable VF loss. The next step major step in expanding the utility of peripapillary imaging is to conduct longitudinal studies to evaluate the ability of these instruments to document RNFL change over time and whether early RNFL structural changes predict the development of VF defects. The rapidly improving technology impedes conducting longitudinal studies because peripapillary measurements collected from prior models are not compatible with measurements from newer models (with the exception of the HRTIII). As such, RNFL thickness measurements from the Stratus OCT are not

comparable with measurements taken from the Cirrus-HD OCT. Furthermore, each new model has a different normative database for comparison. This inherent problem with rapidly evolving technologies also inhibits using imaging derived RNFL baseline thickness measurements to follow glaucoma progression in clinical practice.

Future Study Proposal

With the widespread use of computerized RNFL analysis in the diagnosis and management of glaucoma, it is important for the clinician to understand the data provided in order to accurately utilize the information in glaucoma management. A major limitation of our present study using the time domain Stratus OCT model was the inability to rule-out scan circle decentration as an explanation of the horizontal peak contour displacement. With the spectral domain Cirrus High Definition (HD)-OCT model, it will be possible to eliminate scan circle decentration because the scan circle is digitally created after processing of the RNFL data.

The purpose of this next study will be to evaluate how common significant horizontal peak contour displacement (not due to decentration) from the normative database may be using the spectral domain Cirrus HD-OCT Fast RNFL scan in a practice with glaucoma patients and glaucoma suspects, to explore whether demographic or glaucoma-related variables are associated with this finding and to emphasize the importance of this finding when interpreting OCT data. Our hypothesis is that horizontal peak contour displacement from the normative database observed on the Fast RNFL scan is a common occurrence because there is a range of distribution of peak contours due to anatomical variation, not necessarily related to glaucoma, and this displacement may lead to misclassification as glaucoma under current commercial OCT criteria (comparing an individual's RNFL measurements to a normative database) resulting in over aggressive treatment for glaucoma. Due to time constraints, it is not possible to perform a longitudinal study.

The study design will be a prospective case series of consecutive patients seen at the Yale Eye Center, Department of Ophthalmology and Visual Science, New Haven, CT. The inclusion criteria will be glaucoma patients and glaucoma suspects who undergo a Cirrus HD-OCT Fast RNFL scan between December 2008 and May 2009. Exclusion criteria will include patients under 20 years of age (normative database is not available below this age), a superior or inferior peak contour amplitude < 100 μm (peak of the contour is difficult to identify below this amplitude), and signal strength of less than 6 (analysis algorithms may fail on scans with low signal strength <5). One eye from each subject will be randomly selected for analysis (using the "random sample of cases" function in SPSS), although both eyes will be studied to determine bilaterality of findings, and the most recent test will be chosen for patients who have more than one test. This study is pending approval by the Yale University HIC and conforms to the Declaration of Helsinki research on human subjects and HIPPA.

An experienced technician will obtain the circumpapillary RNFL thickness profile with a Cirrus HD-OCT system (Carl Zeiss Meditec, Dublin, CA) using the Fast RNFL scan pattern. Each study will be evaluated for signal strength, amplitude and horizontal position of the superior and inferior peak contours relative to the aged-matched normative database. The exact horizontal distance between the peaks of the patient's RNFL profile and that of the normative database will be measured digitally using EyeRoute software (Topcon Medical Systems, Inc., Paramus, NJ) which allows measurement of distances in mm, which will then be converted to degrees. A significant horizontal shift of the peak contour will be defined as 20^{o} (1.7mm) or greater nasal or temporal to the corresponding peak contour of the normative database. An eye will be considered to have a clinically

significant horizontal deviation if there is a 20^{o} or greater shift of both the superior and inferior peaks.

Figures

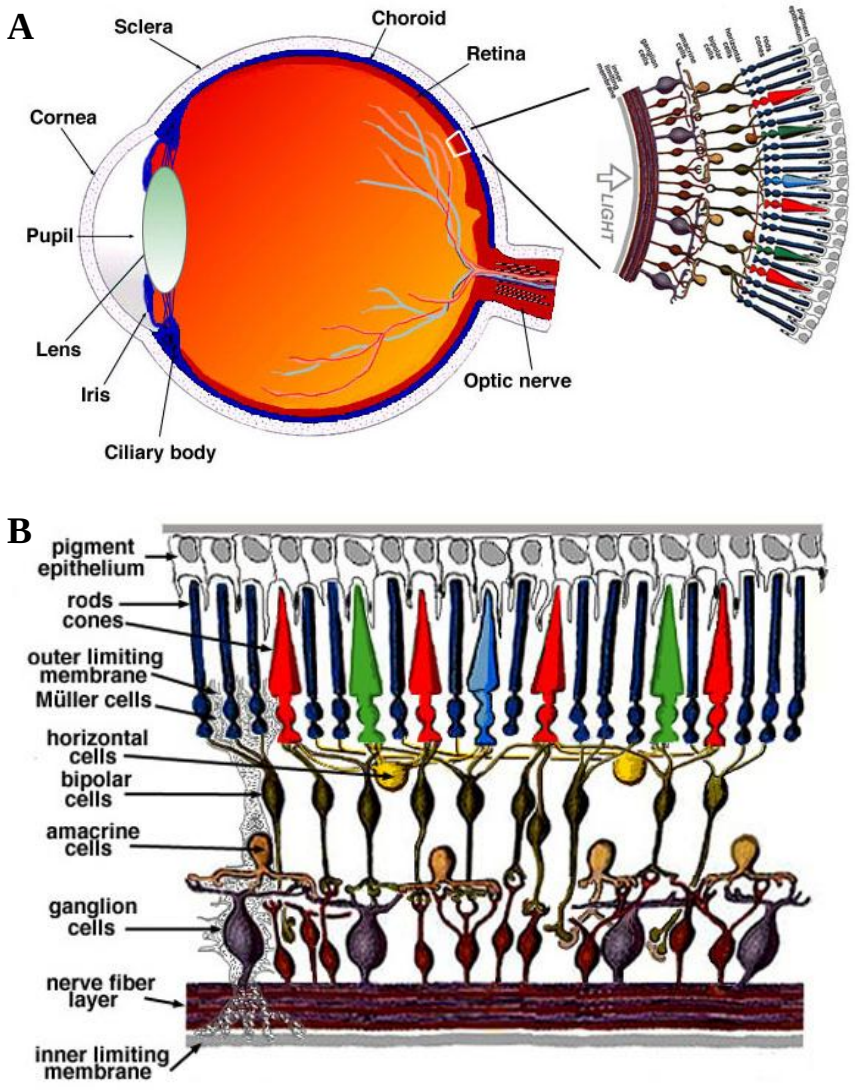

Figure 1: *A. Schematic section through the eye and optic nerve head. *B. Schematic cross-section of the layers of the retina.

*Images A and B are from Webvision: Simple Anatomy of the Retina. John Moran Eye Center University of Utah. 16 Feb. 2008 <http://webvision.med.utah.edu/sretina.html>.

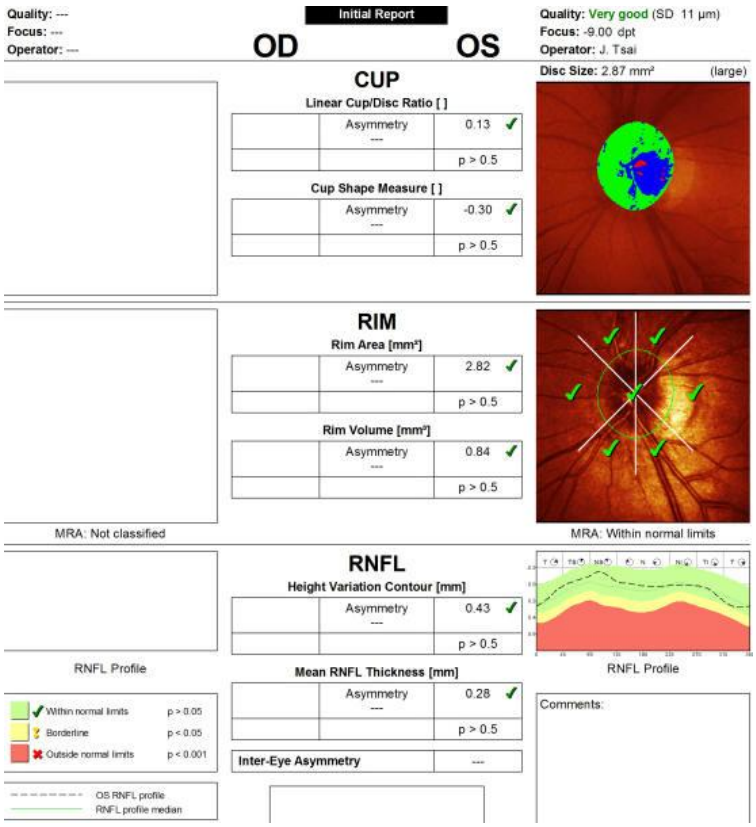

Figure 2: Heidelberg Retina Tomograph (HRT) standard printout in a normal control showing the retinal nerve fiber layer (RNFL) thickness profile (dotted black line) against the age stratified normative database (green, yellow, red) in the bottom right, obtained using a HRTII system.

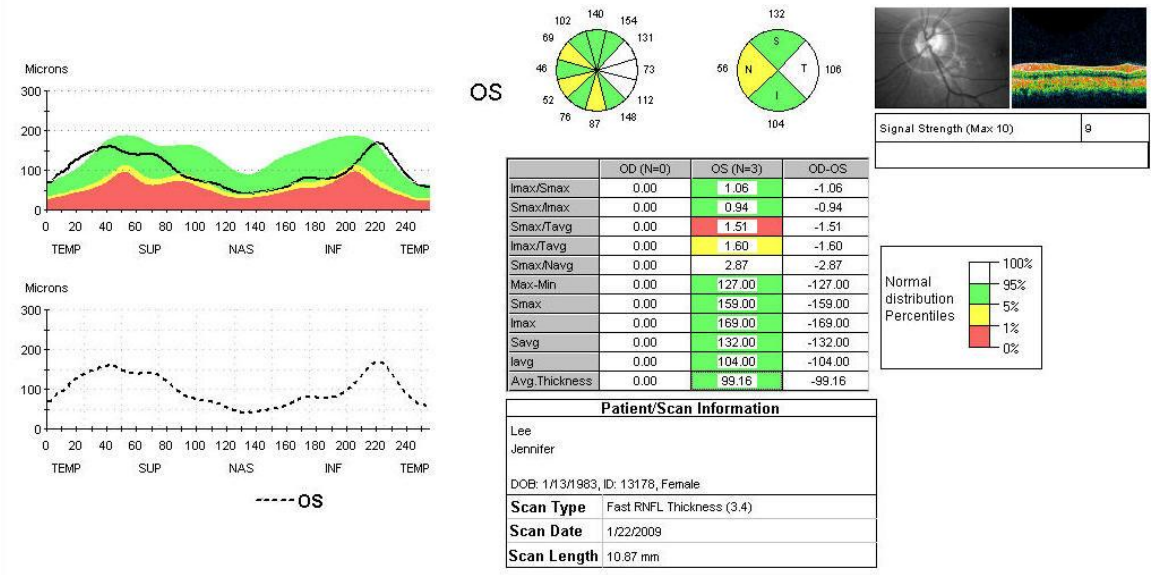

Figure 3: Stratus OCT standard printout in a normal control showing the fundus image with scan circle centration (right corner), peripapillary retinal cross section image (far right corner), and circumpapillary RNFL thickness profile (black line) against age stratified normative database (green, yellow, red) (upper left), obtained using a Stratus OCT 3000 system.

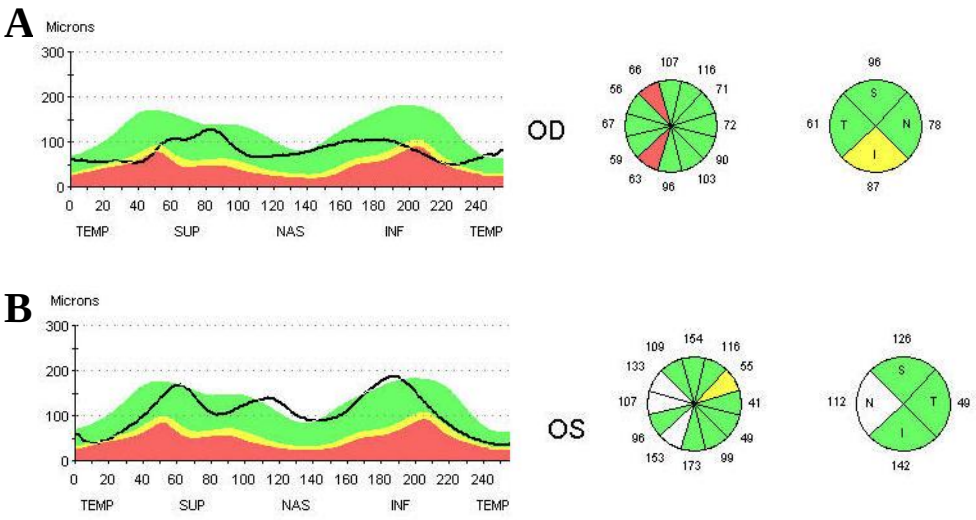

Figure 4: A. Stratus OCT circumpapillary RNFL thickness profile with horizontal deviation* in a glaucoma patient with a cup-disc ratio of 0.9 and documented visual field scotoma (i.e. true glaucoma). B. Stratus OCT circumpapillary RNFL thickness profile with horizontal deviation* in a glaucoma suspect with a cup-disc ratio of 0.3 and no visual field defect (i.e. RNFL thinning possibly due to peak shifts).

*20^{o} or more shift nasal or temporal to the corresponding peak contour of the normative database in both the superior and inferior peaks

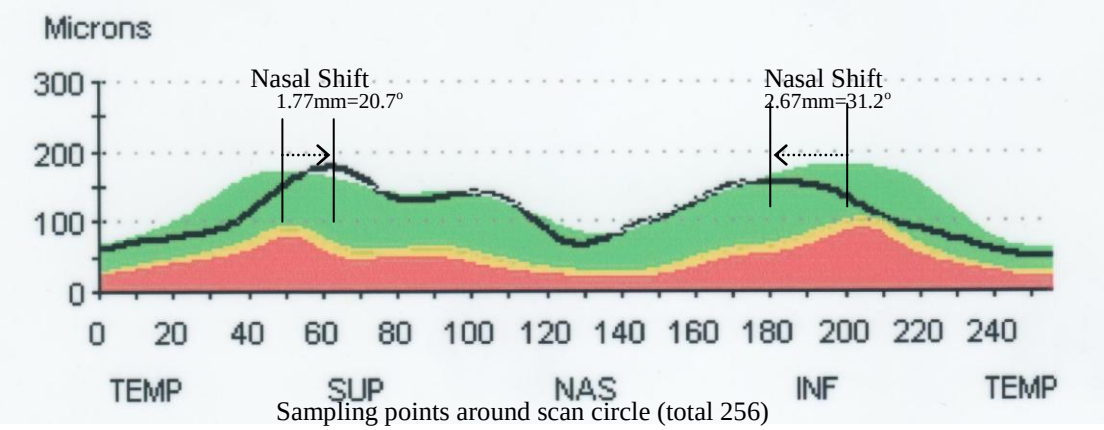

Figure 5: Circumpapillary RNFL thickness profile (black line) against age stratified normative database (green, yellow, red), obtained using a Stratus OCT 3000 system, showing nasal shifts >20^{o} in the superior and inferior peaks, classified as a significant horizontal deviation.

References

1. Smith P. On a case of chronic glaucoma of unusually long duration. 1885. *Ophthalmic Ver*. 4:261-266.

2. Flammer J, Orgul S, Costa VP et al. 2002. The impact of ocular blood flow in glaucoma. *Progress in Retinal Eye Research.* 21:359-393.

3. Von Graefe A. 1857. Über die Iriectomie bei Glaukom und über den glaucomatösen. *Arch Ophthal.* 3:456-555.

4. Yan DB, Coloma FM, Metheetrairut A, et al. 1994. Deformation of lamina cribrosa by elevated intraocular pressure. *Br J Ophthalmol*. 78: 643-648.

5. Weber J, Koll W, Frieglstein GK. 1993. Intraocular pressure and visual field decay in chronic glaucoma. *Ger J Ophthalmol.* 2:165-169.

6. Mozaffarieh M, Grieshaber MC, Flammer J. 2008. Oxygen and blood flow: players in the pathogenesis of glaucoma. *Molecular Vision.* 14:224-233.

7. Gherghel D, Friffiths HR, Hilton EJ, et al. 2005. Systemic reduction in glutathione levels occurs in patients with primary open-angle glaucoma. *Invest Ophthalmol Vis Sci.* 46: 877-883.

8. Izzotti A, Sacca SC, Cartiglia C, et al. 2003. Oxidative deoxyribonucleic acid damage in the eyes of glaucoma patients. *Am J Med.* 114:638-646.

9. Alvarado JA, Murphy C, Juster R. 1984. Trabecular meshwork cellularity in primary open-angle glaucoma and nonglaucomatous normals. *Ophthalmology.* 91:564-579.

10. Sacca SC, Izzotti A, Rossi P, et al. 2007. Glaucomatous outflow pathway and oxidative stress. *Exp Eye Res.* 84:389-399.

11. Sacca SC, Pascotto A, Camicione P. 2005. Oxidative DNA damage in the human trabecular meshwork: clinical correlation in patients with primary open-angle glaucoma. *Arch Ophthalmol.* 123: 1-7.

12. Noske W, Hensen J, Wiederholt M. 1997. Endothelin-1-like immunoreactivity in aqueous humor of patients with primary open-angle glaucoma and cataract. *Graefes Arch Clin Exp Ophthalmol.* 235:551-552.

13. Orgül S, Gugleta K, Flammer J. 1999. Physiology of perfusion as it relates to the optic nerve head. *Surv Ophthalmol*. 43:S17-S26.

14. Chauhan BC, LeVatte TL, Jollimore CA et al. 2004. Model of endothelin-I-induced chronic optic neuropathy in rat. *Investig Ophthalmol Vis Sci.* 45:144-152.

15. Yen TC, Chen YS, King KI, et al. 1989. Liver mitochondrial respiratory function decline with age. *Biochem Biophys Res Commun.* 165:994-1003.

16. Hoyt WF, Newman NM. 1972. The earliest observable defect in glaucoma. *Lancet*. 1:692-693.

17. Sommer A, Katz J, Quigley HA, et al. 1991. Clinically detectable nerve fiber atrophy preceded the onset of glaucomatous field loss. *Arch Ophthalmol*. 109:77.

18. Quigley HA, Addicks EM, Green WR. 1982(a). Optic nerve damage in human glaucoma. *Arch Ophthalmol.* 100:135.

19. Quigley HA and Addicks EM. 1982(b). Quantitative studies of retinal nerve fiber layer defects. *Arch Ophthalmol.* 100:807-814.

20. Townsend KA, Wollstein G, Schuman JS. 2008. Imaging of the retinal nerve fiber layer for glaucoma. *Br J Ophthalmol.* In press.

21. Bowd C, Zangwill LM, Berry CC, et al. 2001. Detecting early glaucoma by assessment of retinal nerve fiber layer thickness and visual function. *Invest Ophthalmol Vis Sci.* 42:1993-2003.

22. Zangwill LM, Bowd C. 2006. Retinal nerve fiber layer analysis in the diagnosis of glaucoma. *Current Opinion in Ophthalmology.* 17: 120-131.

23. Zangwill LM, Chan K, Bowd C, et al. 2004. Heidelberg retina tomography measurements of the optic disc and parapapillary retina for detecting glaucoma analyzed by machine learning classifiers. *Invest Ophthalmol Vis Sci.* 45:3144-3151.

24. Wollstein G, Schuman JS, Price LL, et al. 2004. Optical coherence tomography (OCT) macular and peripapillary retinal nerve fiber layer measurements and automated visual fields. *Am J Ophthalmol.* 138:218-225.

25. Bowd C, Medeiros FA, Zhang Z, et al. 2005. Relevance vector machine and support vector machine classifier analysis of scanning laser polarimetry retinal nerve fiber layer measurements. *Invest Ophthalmol Vis Sci.* 46:1322-1329.

26. Weinreb RN, Shakiba S, Zangwill L. 1995. Scanning laser polarimetry to measure the nerve fiber layer of normal and glaucomatous eyes. *Am J Ophthalmol.* 119:627-636.

27. Lin SC, Kuldev S, Jampel HD, et al. 2007. Optic nerve head and Retinal nerve fiber layer analysis. *Ophthalmology.* 114: 1937-1949.

28. Medeiros FA, Zangwill LM, Bowd C, Weinreb RN. 2004. Comparison of the GDx VCC scanning laser polarimeter, HRT II confocal scanning laser ophthalmoscope, and stratus OCT optical coherence tomograph for the detection of glaucoma. *Arch Ophthalmol.* 122:827–837.

29. Bowd C, Zangwill LM, Weinreb RN. 2003. Association between scanning laser polarimetry measurements using variable corneal polarization compensation and visual field sensitivity in glaucomatous eyes. *Arch Ophthalmol.* 121:961-966.

30. Wollstein G, Garway-Heath DF, Hitchings RA. 1998. Identification of early glaucoma cases with the scanning laser ophthalmoscope. *Ophthalmology.* 105:1557-1563.

31. Huang D, Swanson EA, Lin CP, et al. 1991. Optical coherence tomography. *Science.* 254:1178-1181.

32. Medeiros FA, Zangwill LM, Bowd C, et al. 2005(a). Evaluation of retinal nerve fiber layer, optic nerve head, and macular thickness measurements for glaucoma detection using optical coherence tomography. *Am J Ophthalmol.* 139:44–55.

33. Kanamori A, Nakamura M, Escano MF, et al. 2003. Evaluation of the glaucomatous damage in retinal nerve fiber layer thickness measured by optical coherence tomography. *Am J Ophthalmol.* 135: 513-520.

34. Leung CK, Kong KK, Chan WM, et al. 2005(a). Comparative study of retinal nerve fiber layer measurements by Stratus OCT and GDx VCC, II: structure/function regression analysis in glaucoma. *Invest Ophthalmol Vis Sci*. 46:3702-3711.

35. Nouri-Mahdavi K, Hoffman D, Tannenbaum DP, et al. 2004. Identifying early glaucoma with optical coherence tomography. *Am J Ophthalmol.* 137:228-235.

36. Bagga H, Greenfield DS, Feuer W, et al. 2003. Scanning laser polarimetry with variable corneal compensation and optical coherence tomography in normal and glaucomatous eyes. *Am J Ophthalmol*. 135: 521-529.

37. Essock EA, Sinai MJ, Bowd C, et al. 2003. Fourier analysis of optical coherence tomography and scanning laser polarimetry retinal nerve fiber layer measurements in the diagnosis of glaucoma. *Arch Ophthalmol.* 121:1238-1245.

38. Hoffman EM, Bowd C, Medeiros FA, et al. 2005. Agreement among 3 optical imaging methods for the assessment of optic disc topography. *Ophthalmology.* 112:2149-2156.

39. Leung CK , Chan WM, Chong KK, et al. 2005(b). Comparative study of retinal nerve fiber layer measurement by Stratus OCT and GDx VCC, I: correlation analysis in glaucoma. *Invest Ophthalmol Vis Sci*. 46:3214–3220.

40. Reus NJ, Lemij HG. 2005. Relationships between standard automated perimetry, HRT confocal scanning laser ophthalmoscopy, and GDx VCC scanning laser polarimetry. *Invest Ophthalmol Vis Sci.* 46:4182-4188.

41. Schuman JS, Wollstein G, Farra T, et al. 2003. Comparison of optic nerve head measurements obtained by optical coherence tomography and confocal scanning laser ophthalmoscopy. *Am J Ophthalmol.* 135:504-512.

42. Artes PH, Chauhan BC. 2005. Longitudinal changes in visual field and optic disc in glaucoma. *Prog Retina Eye Res.* 24:333-354.

43. Nicolela MT, McCormick TA, Drance SM, et al. 2003. Visual field and optic disc progression in patients with different types of optic disc damage. A longitudinal prospective study. *Ophthalmology.* 110:2178-2184.

44. Wollstein G, Schuman JS, Price LL, et al. 2005. Optical coherence tomography longitudinal evaluation of retinal nerve fiber layer thickness in glaucoma. *Arch Ophthalmol.* 123:464-470.

45. Chauhan BC, McCormick TA, Nicolela MT, LeBlanc RP. 2001. Optic disc and visual field changes in a prospective longitudinal study of patients with glaucoma: comparison of scanning laser tomography with conventional perimetry and optic disc photography. *Arch Ophthalmol.* 119:1492–1499.

46. Zangwill LM, Weinreb RN, Beiser JA, et al. 2005. Baseline topographic optic disc measurements are associated with the development of primary open-angle glaucoma: the Confocal Scanning Laser Ophthalmoscopy Ancillary Study to the Ocular Hypertension Treatment Study. *Arch Ophthalmol.* 123: 1188–1197.

47. Noecker,RJ. 2007. Interpreting Progression Analysis Software: The HRT 3. *Glaucoma Today.* Nov/Dec: 44-47.

48. Mohammadi K, Bowd C, Weinreb RN, et al. 2004. Retinal nerve fiber layer thickness measurements with scanning laser polarimetry predict glaucomatous visual field loss. *Am J Ophthalmol.* 138:592–601.

49. Lalezary M, Medeiros FA, Weinreb RN, et al. 2006. Baseline Optical Coherence Tomography Predicts the Development of Glaucomatous Change in Glaucoma Suspects. *Am M Ophthalmol.* 142: 576-582.

50. Gordon MO, Beiser JA, Brandt JD, et al. 2002. The Ocular Hypertension Treatment Study: baseline factors that predict the onset of primary open-angle glaucoma. *Arch Ophthalmol.* 120:714-720.

51. Medeiros FA, Weinreb RN, Sample, PA, et al. 2005(b). Validation of a predictive model to estimate the risk of conversion from ocular hypertension to glaucoma. *Arch Ophthalmol.* 123:1351-1360.

52. Kim TW, Zangwill LM, Bowd C, et al. 2007. Retinal nerve fiber layer damage as assessed by optical coherence tomography in eyes with a visual field defect detected by frequency doubling technology perimetry but not by standard automated perimetry. *Ophthalmology*. 114:1053-1057.

53. Chen TC, Zeng A, Sun W, et al. 2008. Spectral Domain Optical Coherence Tomography and Glaucoma. *Int Ophthalmol Clin.* 48:29-45.

54. Greenfield, DS and Weinreb RN. 2008. Role of optic nerve imaging in glaucoma clinical practice and clinical trails. *Am J Ophthalmol.* 145:598-603.

55. Weinreb RN, Greve EL. 2004. *Glaucoma diagnosis.* Amsterdam: Kugler Publications. 155-157pp.

56. Schuman JS, Hee MR, Puliafito CA, et al. 1995. Quantification of nerve fiber layer thickness in normal and glaucomatous eyes using optical coherence tomography. *Arch Ophthalmol.* 113:586-96.

57. Hee MR, Izatt JA, Swanson EA, et al. 1995. Optical coherence tomography of the human retina. *Arch Ophthalmol.* 113:325-332.

58. Gabriele ML, Ishikawa H, Wollstein G, et al. 2007. Peripapillary nerve fiber layer thickness profile determined with high speed, ultrahigh resolution optical coherence tomography high-density scanning. *Invest Ophthalmol Vis Sci.* 48:3154-3160.

59. Vizzeri G, Bowd C, Medeiros FA, et al. 2008. Effect of improper scan alignment on retinal nerve fiber layer thickness measurements using Stratus optical coherence tomograph. *J Glaucoma.* 17:341-349.

60. Gabriele ML, Ishikawa H, Wollstein G, et al. 2008. Optical coherence tomography scan circle location and mean retinal nerve fiber layer measurement variability. *Invest Ophthalmol Vis Sci.* 49:2315-2321.

61. Ghadiali Q, Hood DC, Lee C, et al. 2008. An analysis of normal variations in retinal nerve fiber layer thickness profiles measured with optical coherence tomography. *J Glaucoma.* 17:333-340.